Structural Engineering and Mechanics, Vol.1, No.1 (1993) 103-118
DOI: http://dx.doi.org/10.12989/sem.1993.1.1.103

Vibration of elastic and viscoelastic multilayered spaces

P. Karasudhi † and Y.C. Liu ‡

School of Civil Engineering, Asian Institute of Technology, Bangkok 10501, Thailand

Abstract. The near field is discretized into finite elements, and the far field into infinite elements. Closed form far-field solutions to three fundamental problems are used as the shape functions of the infinite elements. Such infinite elements are capable of transmitting all surface and body waves. An efficient scheme to integrate numerically the stiffness and mass matrices of these elements is presented. Results agree closely with those obtained by others.

Key words: attenuations; body waves; elasticity; far field; finite elements; half space; impedance; infinite elements; outgoing waves; near field; P-waves; radiation; shape functions; S-waves; surface wave; vibration; viscoelasticity; wavenumbers.

1. Introduction and nomenclature

1.1. Discretization of material domains

Analytical methods become impractical if not impossible when extended to load transfer problems and/or multilayered half spaces. Several numerical methods have been developed to bypass such difficulties. At the present stage of development, the most efficient numerical algorithm seems to be the one that involves infinite elements for the far field and finite elements for the near field, as shown in Fig. 1 (a). The near field, consisting of the partially embedded body and a finite region of the half space around it, is discretized into conventional finite elements. The far field covering the rest of the half space is discretized into infinite elements. Near the surface of the half space are horizontal infinite elements (HE), while the remainder of the far field is occupied by radiating infinite elements (RE). Every infinite element, more clearly shwon in Fig. 1 (b), has nodes only on the interface between the near field and the far field. Rajapakse and Karasudhi (1986) for homogeneous isotropic elastic half space assumed that the shape functions of the infinite elements have exponential forms of attenuation. More rationally, far-field displacement functions of the three fundamental problems, to be described in the next sections, should be used as the shape functions of infinite element nodal lines as indicated in Fig. 1 (a). Symbols for Cartesian, cylindrical and spherical coordinates are defined in Fig. 2.

† Professor and Dean
‡ Senior Research Associate

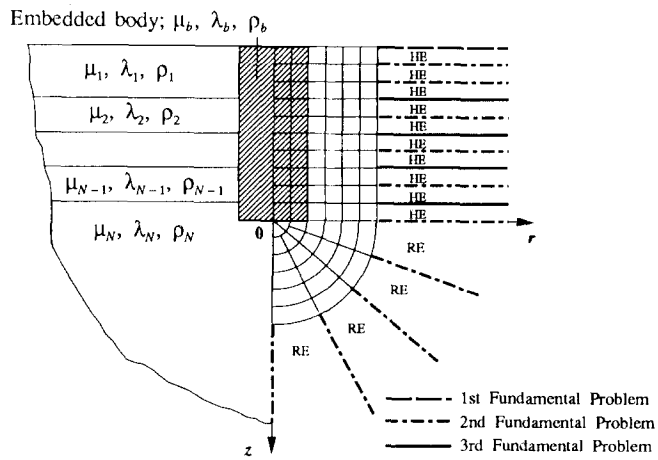

(a) A bar patrially embedded inside a multilayered half space.

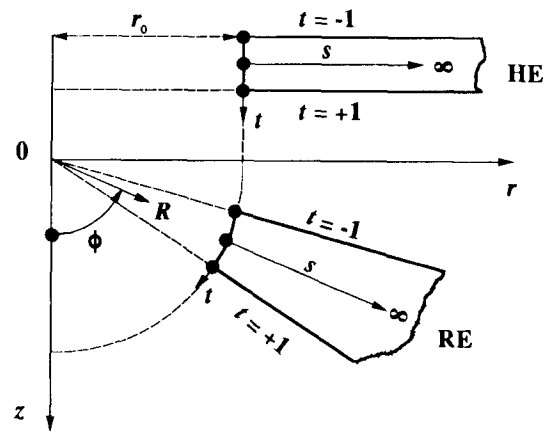

(b) Infinite elements *HE* and *RE*, and natural coordinates s and t.

Fig. 1 Discretization of material domains.

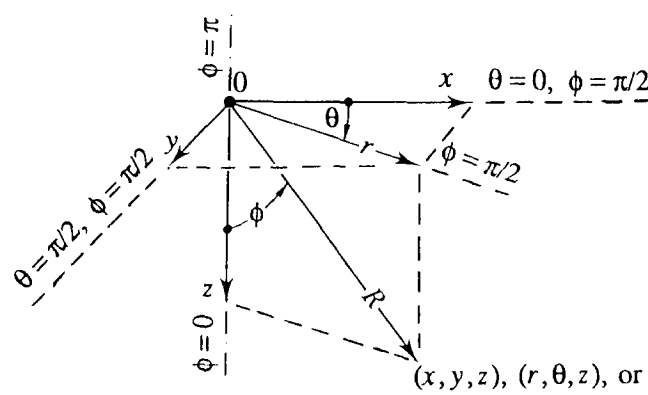

Fig. 2 Cartesian (x, y, z), cylindrical (r, θ, z) and spherical (R, ϕ, θ) coordinates.

1.2. Fundamental problems

Three fundamental problems were considered by Karasudhi and Liu (1992): a homogeneous half space, a homogeneous full space, and two different half spaces perfectly bonded together. The Cartesian displacement components are denoted by u, v, and w, respectively; and the cylindrical displacement components are u_r , u_θ and u_z ($\equiv w$), respectively. In the second fundamental problem, the homogeneous full space is treated as two half spaces bonded together.

Plane problems are those of two-dimensional (2-D) spaces. The xy-plane is used as the plane of reference, the x-dimension is infinite, i.e. $-\infty < x < \infty$, while the y-dimension is constantly finite or infinite. For isotropic *in-plane* problems, w vanishes, while u and v are functions of x and y only, independent of z. In isotropic *antiplane* problems, u and v vanish, while w (x, y) is the only non-vanishing displacement component. In the first fundamental problem, the x-axis is put on the surface of the homogeneous half plane; so, $0 \leq y < \infty$. In the second and third fundamental problems, the $x-$axis is at the interface where the two half planes are perfectly bonded together; so, $0 \leq y < \infty$ and $0 \geq y > -\infty$ for the underlying and overlying half planes, respectively. Unless specified otherwise, subscripts 2 and 1 are used to denote such respective half planes.

In a three-dimensional (3-D) space, the x and y-dimensions are infinite, i.e. $0 \leq r < \infty$, while the z-dimension is constantly finite or infinite. For isotropic axisymmetric problems, u_θ vanishes, while u_r and u_z are functions of r and z only, independent of θ. In isotropic *pure torsion* problems, u_r and u_z vanish, while $u_\theta (r, z)$ is the only non-vanishing displacement-component. In a general 3-D problem, there are three non-vanishing displacement components; u_r (r, θ, z), u_θ (r, θ, z), and u_z (r, θ, z). In the first fundamental problem, the x and y-axes are put on the suface of the homogeneous half space; so $0 \leq z < \infty$. In the second and third fundamental problems, the x and y-axes are at the interface where the two half spaces are perfectly bonded together; so, $0 \leq z < \infty$ and $0 \geq z > -\infty$ for the underlying and overlying half spaces, respectively. Unless specified otherwise, subscripts 2 and 1 are used to denote such respective half spaces.

1.3. Problem numbers

In each fundamental problem, the load is of unit intensity and concentrated at the origin 0 of the reference coordinate systems. In Tables 1 and 2; the usual explicity symbols for stress components are adopted, δ denotes the Dirac-delta function, the superscript$^{(1)}$ denotes the first derivative, 0^+ stands for an infinitesimal positive quantity, the only inhomogeneous boundary condition for each case is listed, and a 'mode type' is assigned to each case. Later (in Tables 4 to 7), each problem will be referred to by three numerals separated by periods; the first numeral stands for the fundamental problem number, the second for the dimensions of the space, and the third for the mode type.

Table 1 Mode types for plane (2-D) problems.

Fundamental Problems	Unit Load Type	Unit Load Direction	The Only Inhomogeneous Boundary Condition	Mode Types
1	Force	y	$\sigma_{yy}(x, 0) = -\delta(x)$	1
	Force	x	$\sigma_{yy}(x, 0) = -\delta(x)$	2
	Force	z	$\sigma_{yz}(x, 0) = -\delta(x)$	3
	Moment	y	$\sigma_{yz}(x, 0) = -\delta^{(1)}(x)$	4
2 and 3	Force	y	$\sigma_{yy1}(x, 0) - \sigma_{yy2}(x, 0) = \delta(x)$	1
	Force	x	$\sigma_{yy1}(x, 0) - \sigma_{yx2}(x, 0) = \delta(x)$	2
	Force	z	$\sigma_{yz1}(x, 0) - \sigma_{yz2}(x, 0) = \delta(x)$	3
	Moment	y	$\sigma_{yz1}(x, 0) - \sigma_{yz2}(x, 0) = \delta^{(1)}(x)$	4

Table 2 Mode types for three-dimensional (3-D) problems.

Fundamental Problems	Unit Load Type	Unit Load Direction	The Only Inhomogeneous Boundary Condition $\times 2\pi r$	Mode Types
1	Force	z	$\sigma_{zz}(r, \theta, 0) = -\delta(r-0^+)$	5
	Force	x	$\sigma_{zx}(r, \theta, 0) = -\delta(r-0^+)$	6
	Moment	z	$\sigma_{z\theta}(r, \theta, 0) = \delta^{(1)}(r-0^+)$	7
2 and 3	Force	z	$\sigma_{zz1}(r, \theta, 0) - \sigma_{zz2}(r, \theta, 0) = \delta(r-0^+)$	5
	Force	x	$\sigma_{zx1}(r, \theta, 0) - \sigma_{zx2}(r, \theta, 0) = \delta(r-0^+)$	6
	Moment	z	$\sigma_{z\theta 2}(r, \theta, 0) - \sigma_{z\theta 1}(r, \theta, 0) = \delta^{(1)}(r-0^+)$	7

2. Far-field solutions to fundamental problems

2.1. Outgoing and attenuating waves

Displacement components in harmonic vibration problems take the forms

$$F(x, y)\exp(i\omega t) \quad \text{and} \quad F(r, \theta, z)\exp(i\omega t)$$

for 2-D and 3-D spaces, respectively; where ω is the frequency, t=time, and $i=\sqrt{-1}$. The inverse integral trasforms involved (Karasudhi 1991) are; for isotropic elastic planes,

$$\int_0^\infty f(\eta, \alpha_p, \alpha_s)\left[e^{-\alpha_p y}, e^{-\alpha_s y}\right]\cos\eta x d\eta, \quad \int_0^\infty f(\eta, \alpha_p, \alpha_s)\left(e^{-\alpha_p y}, e^{-\alpha_s y}\right)\sin\eta x d\eta \quad (1a, b)$$

and for isotropic elastic 3-D spaces,

$$\int_0^\infty f(\eta, \alpha_p, \alpha_s)\left(e^{-\alpha_p z}, e^{-\alpha_s z}\right) J_m(\eta r)d\eta \quad (2)$$

where J_m is a Bessel function of the first kind, and

$$\alpha_p(\eta) = +\sqrt{\eta^2 - \eta_p^2}, \quad \alpha_s(\eta) = +\sqrt{\eta^2 - \eta_s^2} \quad (3a, b)$$

in which

$$\eta_p = \frac{a\omega}{c_p}, \quad \eta_s = \frac{a\omega}{c_s}, \quad c_p = \sqrt{\frac{\lambda+2\mu}{\rho}}, \quad c_s = \sqrt{\frac{\mu}{\rho}} \quad (4a\text{-}d)$$

a is a positive real constant of length dimension, η_p and η_s are dimensionless pressure and shear wavenumbers respectively, c_p and c_s are pressure and shear wave speeds respectively, λ and μ are Lamés constants, and ρ is the mass density. Together P-waves (P for pressure) and S-waves (S for shear) are called body waves. A surface wave exists, when f assumes the quotient form

$$f(\eta, \alpha_p, \alpha_s) = \frac{g(\eta)}{F_R(\eta)} \tag{5}$$

and if the root of $F_R(\eta)$ exists at $\eta = \eta_R$. For the first fundamental in-plane and 3-D problems,

$$F_R(\eta) \equiv (2\eta^2 - \eta_s^2)^2 - 4\eta^2 \alpha_p(\eta)\, \alpha_s(\eta) = 0 \tag{6}$$

It can be shown that $\eta_R > \eta_s > \eta_p \geq 0$. For the third fundamental in-plane and 3-D problems,

$$\begin{aligned} F_R(\eta) \equiv{}& \eta^2(\eta^2 - \beta_1 \eta_{s1}^2 - \beta_2 \eta_{s2}^2)^2 + \eta^2 \alpha_{p1}\alpha_{p2}\alpha_{s1}\alpha_{s2} - \alpha_{p1}\alpha_{s1}(\eta^2 - \beta_2 \eta_{s2}^2)^2 \\ & - \alpha_{p2}\alpha_{s2}(\eta^2 - \beta_1 \eta_{s1}^2)^2 + \beta_1 \beta_2 \eta_{s1}^2 \eta_{s2}^2 (\alpha_{p1}\alpha_{s2} + \alpha_{p2}\alpha_{s1}) = 0 \end{aligned} \tag{7}$$

where

$$\beta_1 = \frac{1}{2(1-\beta_4)}, \quad \beta_2 = \frac{1}{2(\beta_4 - 1)}, \quad \beta_3 = \left[\frac{c_{s2}}{c_{s1}}\right]^2, \quad \beta_4 = \frac{\mu_2}{\mu_1} \tag{8a-d}$$

Stoneley (1924) made a through investigation on the subject, thus gained the recognition in having it named as the *Stoneley wave.* Koppe (1948) solved equation (7) numerically and concluded that

$$\eta_{s1},\ \eta_{s2} < \eta_R < \eta_{Ri} \tag{9}$$

where η_{Ri} is the greater Rayleigh wavenumber among those obtained separately by solving equation (6) for each of the constituent homogeneous half planes. There exists at the most one Stoneley wave. The condition for such existence, found by Cagniard (1962), can be written for the case where $\beta_3 < 1$ as

$$-(\beta_3+\beta_4-2)^2 + (\beta_4-2)^2 [(1-\beta_3\gamma_1^2)(1-\beta_3)]^{1/2} + \beta_3\beta_4 [(1-\gamma_2^2)(1-\beta_3)]^{1/2} < 0 \tag{10}$$

Table 3 Wavenumbers for far field in elastic problems.

	Fundamental Problems	Wavenumbers	
		Body	Surface
1	In-plane u, v	η_p, η_s	η_R
	Antiplane w	η_s	None
	3-D u_r, u_z	η_p, η_s	η_R
	u_θ	η_s	None
2	In-plane u, v	η_p, η_s	None
	Antiplane w	η_s	None
	3-D u_r, u_z	η_p, η_s	None
	u_θ	η_s	None
3	In-plane u, v	$\eta_{p1}, \eta_{s1}, \eta_{p2}, \eta_{s2}$	η_R or none
	Antiplane w	η_{s1}, η_{s2}	None
	3-D u_r, u_z	$\eta_{p1}, \eta_{s1}, \eta_{p2}, \eta_{s2}$	η_R or none
	u_θ	η_{s1}, η_{s2}	None

where $\gamma = c_s/c_p$. The existence of body and surface waves for the field (i.e. where x or r is large) in elastic fundamental problems is summarized in Table 3.

For isotropic viscoelastic solids, μ, λ, c_p and c_s are complex function of ω with both real and imaginary parts positive, i.e.

$$\mu \equiv \bar{\mu}(1+i\beta), \quad \lambda \equiv \bar{\lambda}(1+i\beta^*), \quad c_s \equiv \bar{c}_s(1+i\beta_s), \quad c_p \equiv \bar{c}_p(1+i\beta_p) \tag{11a-d}$$

The body wavenumbers given by equations (4a, b) are complex, with positive real parts but negative imaginary parts, i.e.

$$\zeta_p = \eta_p - i\xi_p, \quad \zeta_s = \eta_s - i\xi_s \tag{12a, b}$$

Equations (3) become, respectively,

$$\alpha_p(\eta) = \sqrt{\eta^2 - \zeta_p^2}, \quad \alpha_s(\eta) = \sqrt{\eta^2 - \zeta_s^2} \tag{13a, b}$$

Replacing η by ζ in equation (6) or (7) and solving for its root, the surface wavenumber can be obtained in a similar form as of a body wavenumber, i.e.

$$\zeta_R = \eta_R - i\xi_R \tag{14}$$

A wave, outgoing as x increases, has a factor $\exp(-i\eta x)$; while attenuations due to material properties and geometry are represented by factors $\exp(-\zeta x)$ and x^{-n}, respectively, where n is non-negative. In elastic solids, there is no material attenuation since

$$\xi_p = \xi_s = \xi_R = 0 \tag{15a, b, c}$$

2.2. 2-D fundamental problems

For fundamental plane (2-D) problems, the C.P.V. (Cauchy's principal value) of each of the infinite integrals defined by equations (1), with $y=0$ but large x, can be obtained in outgoing and attenuating wave forms as a combination of

$$x^{-n}\exp(-i\zeta_p x), \quad x^{-n}\exp(-i\zeta_s x), \quad \exp(-i\zeta_R x), \tag{16a, b, c}$$

The geometric attenuation (or radiation) of the surface wave is in the order of x^{-0}, i.e. no radiation The P-wave radiation and the S-wave radiation for each problem number (assigned in Section 1.3) are as presented in Table 4.

2.3. 3-D fundamental problems

For fundamental 3-D problems, the C.P.V. of each of the infinite integrals defined by equation (2), with $z=0$ but large r, can be obtained as a combination of

$$r^{-n}\exp(-i\zeta_p r), \quad r^{-n}\exp(-i\zeta_s r), \quad r^{-1/2}\exp(-i\zeta_R r) \tag{17a, b, c}$$

The radiation of the surface wave is in the order of $r^{-1/2}$. The body wave radiation for each problem number (Section 1.3) are as presented in Table 5.

Table 4 Body wave radiation for plane (2-D) problems.

Problems	Displacements	P-waves	S-waves
1.2.1	u, v	$x^{-3/2}$	$x^{-3/2}$
1.2.2	u, v	$x^{-3/2}$	$x^{-3/2}$
1.2.3	w	-	$x^{-1/2}$
1.2.4	w	-	$x^{-1/2}$
2.2.1	u by (1.2.1)*	$x^{-3/2}$	$x^{-3/2}$
	v	$x^{-3/2}$	$x^{-1/2}$
2.2.2	u	$x^{-1/2}$	$x^{-3/2}$
	u by (1.2.2)*	$x^{-3/2}$	$x^{-3/2}$
2.2.3	w	-	$x^{-1/2}$
2.2.4	w	-	$x^{-1/2}$
3.2.1	u, v	$x^{-3/2}$	$x^{-3/2}$
3.2.2	u, v	$x^{-3/2}$	$x^{-3/2}$
3.2.3	w	-	$x^{-3/2}$
3.2.4	w	-	$x^{-3/2}$

( )* = substitute problem, since actual problem gives trivial component.

Table 5 Body wave radiation for 3-D problems.

Problems	Displacements	P-waves	S-waves
1.3.5	u_r, u_z	r^{-2}	r^{-2}
1.3.6	u_r, u_z	r^{-2}	r^{-2}
	u_θ	-	r^{-2}
1.3.7	u_θ	-	r^{-1}
2.3.5	u_r by (1.3.5)*	r^{-2}	r^{-2}
	u_z	r^{-2}	r^{-1}
2.3.6	u_r	r^{-1}	r^{-2}
	u_z by (1.3.6)*	r^{-2}	r^{-2}
	u_θ	-	r^{-1}
2.3.7	u_θ	-	r^{-1}
3.3.5	u_r, u_z	r^{-2}	r^{-2}
3.3.6	u_r, u_z	r^{-2}	r^{-2}
	u_θ	-	r^{-2}
3.3.7	u_θ	-	r^{-2}

( )* = substitute problem, since actual problem gives trivial component.

2.4. Underlying half plane

Results for large r inside the underlying half plane of a multilayered plane can be obtained easily by setting, in the second fundamental problems, the x'-axis of another coordinate system (x', y') to coincide with a certain r-direction. Since such results happen to be at $y' = 0$, they can be readily taken form Section 2.2. Displacement components for each problem number (Section 1.3) are listed in Table 6.

Table 6 Plane (2-D) problems for large r.

Problems	Displacements, $x' = r$
2.2.1	$u_r(r, \theta) = \sin\theta\, u'^{(x')}(x', 0)$
	$u_\theta(r, \theta) = \cos\theta\, v'^{(y')}(x', 0)$
2.2.2	$u_r(r, \theta) = \cos\theta\, u'^{(x')}(x', 0)$
	$u_\theta(r, \theta) = -\sin\theta\, v'^{(y')}(x', 0)$
2.2.3	$w(r, \theta) = w'^{(z')}(x', 0)$
2.2.4	$w(r, \theta) = \cos\theta\, w'^{(y')}(x', 0)$

$^{(x')}$ = due to unit load in x'-direction, etc.

2.5. Underlying half space

Results for a large spherical radial coordinate R inside the underlying half space of a multilayered 3-D space can be obtained easily by setting, in the second fundamental problems, the x'-axis of another coordinate system (x', y', z') to coincide with a certain R-direction. Since such results happen to be at $z' = 0$, they can be readily taken from Section 2.3. Displacement components for each problem number (Section 1.3) are listed in Table 7.

Table 7 3-D problems for large R.

Problems	Displacements, $r' = R$
2.3.5	$u_R(R, \phi, \theta) = \cos\phi u_{r'}^{(x')}(r', 0, 0)$
	$u_\phi(R, \phi, \theta) = -\sin\phi u_{z'}^{(z')}(r', 0, 0)$
2.3.6	$u_R(R, \phi, \theta) = \cos\theta\, \sin\phi u_{r'}^{(x')}(r', 0, 0)$
	$u_\phi(R, \phi, \theta) = \cos\theta\, \cos\phi u_{z'}^{(z')}(r', 0, 0)$
	$u_\theta(R, \phi, \theta) = -\sin\phi u_{\theta'}^{(y')}(r', 0, 0)$
2.3.7	$u_\theta(R, \phi, \theta) = \sin\phi u_{\theta'}^{(z')}(r', 0, 0)$

$^{(x')}$ = due to unit load in x'-direction, etc.
ϕ = an angular spherical coordinate.

3. Infinite elements and solution scheme

3.1. Infinite element shape functions

The far-field displacement function of the three fundamental problems obtained in Sections 2.3 and 2.5 are used as the shape functions of infinite element nodal lines as indicated in Fig. 1 (a); i.e. the first fundamental problem is used at the surface of the half space, the second in the interior of any homogenious domain, and the third at the interface between two domains of different properties.

Only the case of 3-D problems will be presented here to illustrate the proposed algorithm. In accordance with the definition of *natural coordinates* (s, t) as in Fig. 1 (b), we can write, for HE as,

$$r = r_0 + s, \qquad z = \sum_j L_j(t)\, z_j \tag{18a, b}$$

and for RE as,

$$R = r_0 + s, \qquad \phi = \sum_j L_j(t)\, \phi_j \tag{19a, b}$$

where $L_j(t)$ is the Languagian polynomial corresponding to the nodal line j, and r_0 is the radius of the near field finite element mesh as shown in Fig. 1 (b). Adopting three nodes for each infinite element, the expression of any displacement component y is in terms of the natural coordinates as follows

$$y(s, t) = \sum_{m=1}^{3} \sum_{n=1}^{s_m} L_m(t)\, f_{mn}(s)\, a_{mn} \tag{20}$$

where S_m is number of waves at the node m, f_{mn} is the shape function for the wave n at the node m, and a_{mn} are unknown variables to be determined.

To couple infinite element with the conventional finite elements, it is necessary to find the relationship between the nodal displacements y_m and a_{mn} of each infinite element. In view of equation (20), y_m can be expressed as

$$y_m = \sum_{n=1}^{s_m} f_{mn}^0\, a_{mn}, \quad (m = 1, 2, 3) \tag{21}$$

where

$$y_1 = y(0, -1), \quad y_2 = y(0, 0), \quad y_3 = y(0, 1), \quad f_{mn}^0 = f_{mn}(0) \tag{22a-d}$$

Solving equation (21) for a_{m1} leads to

$$a_{m1} = (f_{m1}^0)^{-1} \left[y_m - \sum_{n=2}^{s_m} f_{mn}^0\, a_{mn} \right], \quad (m = 1, 2, 3) \tag{23}$$

Substituting the equation above into equation (20) yields

$$y = \sum_{m=1}^{3} L_m \left\{ f_{m1}\, (f_{m1}^0)^{-1} y_m + \sum_{n=2}^{s_m} [\, f_{mn} - f_{m1}\, (f_{m1}^0)^{-1} f_{mn}^0 \,]\, a_{mn} \right\} \tag{24}$$

or

$$y(s, t) = \sum_{m=1}^{3} \sum_{n=2}^{s_m} L_m(t)\, F_{mn}(s)\, \bar{a}_{mn} \tag{25}$$

where

$$F_{mn} = f_{m1}(f_{m1}^0)^{-1}, \qquad (n = 1) \tag{26a}$$

$$= f_{mn} - f_{m1}\, (f_{m1}^0)^{-1} f_{mn}^0, \quad (n \neq 1) \tag{26b}$$

$$\bar{a}_{mn} = y_m, \quad (n = 1) \tag{26c}$$

$$= a_{mn}, \quad (n \neq 1) \tag{26d}$$

Rewriting equation (25) in a more common form,

$$\mathbf{u} = \mathbf{NU} \tag{27}$$

where $\mathbf{N}$ is a matrix of interpolation functions,

$$\mathbf{N} = [\,N_{11}\ N_{12} \cdots N_{1s_1}\ N_{21}\ N_{22} \cdots N_{2s_2}\ N_{31}\ N_{32} \cdots N_{3s_3}\,] \tag{28a}$$

$$\mathbf{U} = [\,\bar{a}_{11}\ \bar{a}_{12} \cdots \bar{a}_{1s_1}\ \bar{a}_{21}\ \bar{a}_{22} \cdots \bar{a}_{2s_2}\ \bar{a}_{31}\ \bar{a}_{32} \cdots \bar{a}_{3s_3}]^T \tag{28b}$$

in which

$$N_{mn} = L_m F_{mn} \tag{29}$$

In view of equation (26), we can get,

$$N_{mn}(0, -1) = 1, \quad (m, n = 1) \tag{30a}$$

$$= 0, \quad (m, n \neq 1) \tag{30b}$$

$$N_{mn}(0, 0) = 1, \quad (m = 2, n = 1) \tag{30c}$$

$$= 0, \quad (m \neq 2, n \neq 1) \tag{30d}$$

$$N_{mn}(0, 1) = 1, \quad (m = 3, n = 1) \tag{30e}$$

$$= 0, \quad (m \neq 3, n \neq 1) \tag{30f}$$

Functions of a displacement component of an infinite element along its nodal lines where $m =$ 1 and 3 are, respectively,

$$y\,(s, -1) = \sum_{n=1}^{s_1} F_{1n}(s)\,\bar{a}_{1n}, \quad y\,(s, 1) = \sum_{n=1}^{s_3} F_{3n}(s)\,\bar{a}_{3n} \tag{31a, b}$$

At any point inside an HE, the displacements are

$$\mathbf{u} = \mathbf{NU} \tag{32}$$

where

$$\mathbf{u} = [\,u_r\ u_z\ u_\theta\,]^T, \qquad \mathbf{N} = [\,N_1\ N_2\ N_3\,] \tag{33a, b}$$

$$\mathbf{U} = [\,\mathbf{a}_{r1}\ \ \mathbf{a}_{z1}\ \ \mathbf{a}_{\theta 1}\ \ \mathbf{a}_{r2}\ \ \mathbf{a}_{z2}\ \ \mathbf{a}_{\theta 2}\ \ \mathbf{a}_{r3}\ \ \mathbf{a}_{z3}\ \ \mathbf{a}_{\theta 3}\,]^T \tag{33c}$$

in which

$$\mathbf{N}_k = \begin{bmatrix} L_k \mathbf{F}_{rk} \cos\theta & 0 & 0 \\ 0 & L_k \mathbf{F}_{zk} \cos\theta & 0 \\ 0 & 0 & L_k \mathbf{F}_{\theta k} \sin\theta \end{bmatrix} \tag{34}$$

At any point inside an RE, the displacements are symbolically the same as in equation (32), but

$$\mathbf{u} = [\,u_R\ u_\phi\ u_\theta\,]^T \tag{35a}$$

$$\mathbf{U} = [\,\mathbf{a}_{R1}\ \ \mathbf{a}_{\phi 1}\ \ \mathbf{a}_{\theta 1}\ \ \mathbf{a}_{R2}\ \ \mathbf{a}_{\phi 2}\ \ \mathbf{a}_{\theta 2}\ \ \mathbf{a}_{R3}\ \ \mathbf{a}_{\phi 3}\ \ \mathbf{a}_{\theta 3}\,]^T \tag{35b}$$

$$\mathbf{N}_k = \begin{bmatrix} L_k \mathbf{F}_{Rk} \cos\theta & 0 & 0 \\ 0 & L_k \mathbf{F}_{\phi k} \cos\theta & 0 \\ 0 & 0 & L_k \mathbf{F}_{\theta k} \sin\theta \end{bmatrix} \tag{35c}$$

In the equations above, which are valid only for certain asymmetric problems, a certain form of displacements as functions of θ is assumed. For axisymmetric problems, $u_\theta = 0$, all functions involved are independent of θ, so these equations should be modified accordingly. Beside such asymmetric and axisymmetric problems, the algorithm should be modified such that there are element nodes at various values of θ.

3.2. *Integration schemes for mass and stiffness matrices*

The mass and stiffness matrices of infinite elements involve the infinite integrals, with respect to r and R, in the form

$$\int_{r_0}^{\infty} r^{-v} \exp(-\zeta r)\, dr \tag{36}$$

where $v = n$ or $n + 1/2$ (n is a positive integer).

For viscoelasticity, ζ is complex with $\Re(\zeta) \equiv \eta > 0$ and $\Im(\zeta) \equiv \xi$, where $\Re$ and $\Im$ denote real and imaginary parts, respectively, of a complex quantity. For $v \neq 0$, integrating by parts successively yields

$$\int_{r_0}^{\infty} r^{-\nu} \exp(-\zeta r)\, dr = \frac{\exp(-\zeta r_0)}{(v-1)\, r_0^{v-1}} \left[1 + \frac{\zeta r_0}{(2-v)} + \cdots + \frac{(\zeta r_0)^{m-1}}{(2-v)(3-v)\cdots(m-v)} \right] + \frac{\zeta^m}{(1-v)(2-v)\cdots(m-v)} \int_{r_0}^{\infty} r^{m-v} \exp(-\zeta r)\, dr \tag{37}$$

For $v = n$, we may stop the successive integration by parts when the remaining integrand is $r^{-1} \exp(-\zeta r)\, dr$, and use

$$\int_{r_0}^{\infty} r^{-1} \exp(-\zeta r)\, dr = E_1(r_0 \zeta) \tag{38}$$

where E_1 is an exponential integral (Abramowitz and Stegun 1964), i.e.

$$E_1(z) = -\gamma - \log z - \sum_{m=1}^{\infty} \frac{(-1)^m z^m}{m\, m!} \tag{39}$$

in which $\gamma = 0.5772156649\cdots$ is the Euler's constant. For $\nu = n + 1/2$, we may stop the integration by parts at the step when the remaining integrand is $r^{-1/2}\exp(-\zeta r)dr$, then note the following identities;

$$\int_{r_0}^{\infty} r^{-1/2} \exp(-\zeta r)\, dr = F_*(\eta, \xi) - \int_0^{r_0} r^{-1/2} \exp(-\zeta r)\, dr \tag{40a}$$

$$F_*(\eta, \xi) = \int_0^{\infty} r^{-1/2} \exp(-\zeta r)\, dr = \left[\frac{\pi}{2} \frac{(\eta^2 + \xi^2)^{1/2} + \eta}{\eta^2 + \xi^2} \right]^{1/2} - \mathrm{i} \left[\frac{\pi}{2} \frac{(\eta^2 + \xi^2)^{1/2} - \eta}{\eta^2 + \xi^2} \right]^{1/2} \tag{40b}$$

where $F_*(\eta, \xi)$ is a Fourier transform (Erdélyi, Magnus, Oberhettinger and Tricomi 1954). The improper integrals over a finite interval in equation (40a), i.e.

$$\int_0^{r_0} r^{-1/2} \exp(-\eta r) \cos\xi r \, dr, \quad \int_0^{r_0} r^{-1/2} \exp(-\eta r) \sin\xi r \, dr \tag{41a, b}$$

can be transformed into proper ones by the transformation $t^2=r$, then can be evaluated by a standard numerical method such as the Simpson's rule. For $\nu=0$, the integral, equation (36), becomes

$$\int_{r_0}^{\infty} \exp(-\zeta r)\, dr = \zeta^{-1}\exp(-\zeta r_0) \tag{42}$$

For elasticity, $\Re(\zeta)\equiv\eta=0$ and $\Im(\zeta)\equiv\zeta\neq 0$. For $\nu=0$, equation (36) becomes

$$\int_{r_0}^{\infty} \exp(-i\xi r)dr = \int_0^{\infty} H(r)\exp(-i\xi r)dr - \int_0^{r_0} \exp(-i\xi r)dr \tag{43a}$$

$$= (i\xi)^{-1}\exp(-i\xi r_0) \tag{43b}$$

where the Fourier transform of the Heaviside step function $H(r)$,

$$\int_0^{\infty} H(r)\exp(-i\xi r)dr = \frac{1}{i\xi} + \pi\delta(\xi) \tag{44}$$

(Hsu 1970) has been applied. Note that equation (43b) is a special case of equation (42). For $\nu=n$, we must stop the successive integration by parts in equation (37) when the remaining integrand is $r^{-1}\exp(-i\xi r)dr$, and use the results

$$\int_{r_0}^{\infty} r^{-1}\cos\xi r dr = -\mathrm{Ci}(r_0\xi), \quad \int_{r_0}^{\infty} r^{-1}\sin\xi r dr = -\mathrm{si}(r_0\xi) \tag{45a, b}$$

where $\mathrm{Ci}(r_0\xi)$ and $\mathrm{si}(r_0\xi)$ are cosine and sine integrals (Abramowitz and Stegun 1964), respectively. For $\nu=n+1/2$, we must stop the integration at the step when the remaining integrand is $r^{-1/2}\exp(-i\xi r)dr$, then employ equations (40, 41) with $\eta=0$.

An overflow in computing $E_1(z)$from equation (39) may arise before its convergence can be realized, especially for large z. It is more practical to adopt the following scheme,

$$\begin{aligned} E_1(z) &= \int_1^{\infty} r^{-1}\exp(-zr)dr \\ &= \int_0^{\infty} r^{-1}(e^{-xr}-1)e^{-iyr}dr + \int_1^{\infty} r^{-1}e^{-iyr}dr - \int_0^{1} r^{-1}(e^{-xr}-1)e^{-iyr}dr \\ &= \frac{1}{2}\log\frac{y^2}{x^2+y^2} - i\frac{y}{x}\arctan + i\frac{\pi}{2} - \mathrm{Ci}(y) + i\,\mathrm{si}(y) - \int_0^{1} r^{-1}(e^{-xr}-1)e^{-iyr}dr \end{aligned} \tag{46}$$

where $z=x+iy$, and the remaining integral on the right-hand side of the last equation is proper. Rational approximations are available for $\mathrm{Ci}(y)$ and $\mathrm{si}(y)$, for $1\leq y<\infty$, as follow,

$$\mathrm{Ci}(y) = f(y)\sin y - g(y)\cos y, \quad \mathrm{si}(y) = -f(y)\cos y - g(y)\sin y \tag{47a, b}$$

where

$$f(y) = \frac{1}{y}\left(\frac{y^4+a_1y^2+a_2}{y^4+a_3y^2+a_4}\right) + \varepsilon_1(y), \quad g(y) = \frac{1}{y^2}\left(\frac{y^4+b_1y^2+b_2}{y^4+b_3y^2+b_4}\right) + \varepsilon_2(y) \tag{47c, d}$$

in which $a_1=7.241163$, $a_2=2.463936$, $a_3=9.068580$, $a_4=7.157433$, $|\varepsilon_1(y)|<2\times10^{-4}$, $b_1=7.547478$, $b_2=1.564072$, $b_3=15.723606$, $b_4=12.723684$, and $|\varepsilon_2(y)|<10^{-4}$. More accurate approximations than these are also available. For $y<1$, one should use the following integrals.

$$\mathrm{Ci}(y)=\gamma+\log y+\int_0^y \frac{\cos r-1}{r}\mathrm{d}r, \quad \mathrm{si}(y)=\int_0^y \frac{\sin r}{r}\mathrm{d}r-\frac{\pi}{2} \tag{48a, b}$$

which are proper.

3.3. Solution scheme for complex simultaneous equations

The stiffness equation of an element can be written as

$$\mathbf{K}^{*e}(\omega)\,\mathbf{U}^e(\omega)=\mathbf{P}^e(\omega) \tag{49}$$

where

$$\mathbf{K}^{*e}(\omega)=\mathbf{K}^e(\omega)-\omega^2\mathbf{M}^e(\omega) \tag{50}$$

$\mathbf{K}^e$, $\mathbf{M}^e$, $\mathbf{U}^e$ and $\mathbf{P}^e$ are stiffness matrix, mass matrix, general nodal displacement vector and equivalent nodal force vector, respectively, of an element. Decomposing every term in equation (49) into its real and imaginary parts leads to

$$(\overset{*e}{\mathbf{K}}_r+i\overset{*e}{\mathbf{K}}_i)(\mathbf{U}_r^e+i\mathbf{U}_i^e)=(\mathbf{P}_r^e+i\mathbf{P}_i^e) \tag{51}$$

where subscripts r and i denote real and imaginary parts, respectively. Equating the real and imaginary parts of the equation above, the following set of real equations are obtained

$$\overset{*e}{\mathbf{K}}_r\mathbf{U}_r^e-\overset{*e}{\mathbf{K}}_i\mathbf{U}_i^e=\mathbf{P}_r^e, \qquad \overset{*e}{\mathbf{K}}_i\mathbf{U}_r^e+\overset{*e}{\mathbf{K}}_r\mathbf{U}_i^e=\mathbf{P}_i^e \tag{52a, b}$$

or

$$\overset{*e}{\mathbf{K}}_c(\omega)\,\mathbf{U}_c^e(\omega)=\mathbf{P}_c^e(\omega) \tag{53}$$

where

$$\overset{*e}{\mathbf{K}}_c(\omega)=\begin{bmatrix} \overset{*e}{\mathbf{K}}_r & -\overset{*e}{\mathbf{K}}_i \\ -\overset{*e}{\mathbf{K}}_i & -\overset{*e}{\mathbf{K}}_r \end{bmatrix}, \qquad \mathbf{U}_c^e(\omega)=\begin{Bmatrix} \mathbf{U}_r^e \\ \mathbf{U}_i^e \end{Bmatrix}, \qquad \mathbf{P}_c^e(\omega)=\begin{Bmatrix} \mathbf{P}_r^e \\ -\mathbf{P}_i^e \end{Bmatrix} \tag{54a, b, c}$$

Since $\overset{*e}{\mathbf{K}}_c(\omega)$ is symmetric, equation (53) can be solved efficiently by any standard algorithm for solving a set of real simultaneous equations.

4. Comparison of results

This paper has been based in parts upon the dissertation of the second author (Liu 1992), whose results for both 2-D and 3-D cases agreed closely with the existing results obtained by others; i.e. Luco and Westmann (1971, 1972), Veletsos and Wei (1971), Veletsos and Verbic (1973), Veletsos and Nair (1974), Keer, Jabali and Chuntaramungkorn (1974), Luco (1974,

an example of the accuracy of the proposed algorithm, the case of a rigid cylindrical foundation embedded in a layered soil deposit is to be considered. The discretization of the material domains into finite and infinite elements is as shown in Fig. 3. The foundation, assumed to be in welded contact with the surrounding soil, had radius $a = 40$ft and length $h_1 = 16$ft. The properties of the soil deposit, consisting of two parallel viscoelastic layers overlying a uniform viscoelastic half space, are listed in Table 8. The foundation is subjected to a force $Q_0 \exp(i\omega t)$ is in x-direction, and a moment $M_0 \exp(i\omega t)$ in the opposite direction to the y-axis. The horizontal, rocking and coupling impedance functions, referred to the center of the base of the foundation, are shown in Fig. 4, agreeing closely with those by Mita and Luco (1987). In addition to those defined in equations (11), new symbols are introduced as the following: h is layer thickness, a subnumeral (i) denotes the ith layer, $\triangle_Q$ is the amplitude of the displacement in the x-direction due to the force Q_0, ϕ_M the rocking angle due to the moment M_0, $\triangle_M$ the displacement due to the moment M_0, and ϕ_Q the angle due to the force Q_0.

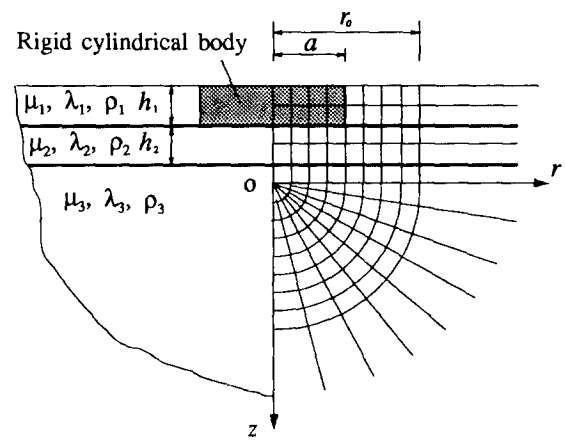

Fig. 3 Element mesh for 3-D problems of a rigid cylindrical body embedded in a visoelastic multilayered half space.

Table. 8 Material properties for layered soil model.

Layer Number	$\bar{c}_s$ ft/sec	$\bar{c}_p$ ft/sec	ρ lb/ft^3	$\beta_s/2$ %	$\beta_p/2$ %	Thickness h, ft
1	980	2400	133	0.5	0.25	16
2	1270	2540	133	0.5	0.25	16
3	1380	2760	133	0.333	0.167	∞

Notes: 1ft = 0.305m, 1lb = 4.448N.

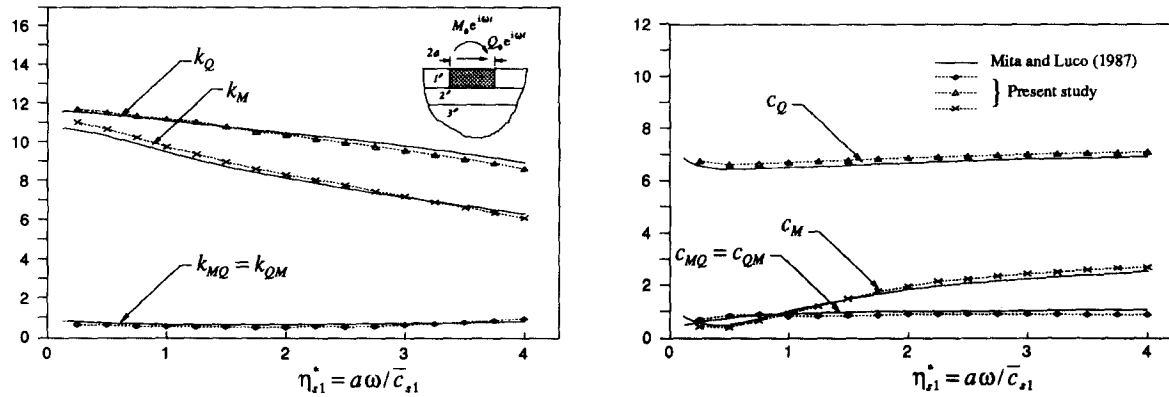

Fig. 4 Horizontal impedance $k_Q + i\eta^*_{s1}\, c_Q \equiv Q_0/(a\bar{\mu}_1 \Delta_Q)$; rocking impedance $k_M + i\eta^*_{s1}\, c_M \equiv M_0/(a^3\bar{\mu}_1\, \phi_M)$; and coupling impedance $k_{MQ} + i\eta^*_{s1}\, c_{MQ} \equiv M_0/(a^2\bar{\mu}_1 \Delta_M) = k_{QM} + i\eta^*_{s1}\, c_{QM} \equiv Q_0/(a^2\bar{\mu}_1 \phi_Q)$.

5. Conclusions

The proposed infinite elements are capable of transmitting all surface and body waves; and satisfy the compatibility, completeness, finiteness and attenuation conditions. An efficient scheme to integrate numerically the stiffness and mass matrices of the elements is presented. With such infinite elements in the far field, the size of the near field being discretized into conventional finite elements can be kept small, the problems have relatively fewer degrees of freedom, and an analyst is provided with an inexpensive solution scheme. The compliance and/or impedance functions obtained by the present algorithm are found to agree closely with analytical results obtained by others.

References

Abramowitz, M. and Stegun, I.A. (eds.) (1965), *Handbook of Mathematical Functions,* Dover Publications, New York, 228-251 and 355-494.

Apsel, R.J. and Luco, J.E. (1987), "Impedance functions for foundations embedded in a layered medium: An integral equation approach", *Earthquake Eng. Struct. Dyn.,* **15,** 213-231.

Cagniard, L. (1962), *Reflection and Refraction of Progressive Seismic Waves,* E.A. Flinn and C.H. Dix (translated and revised), McGraw-Hill, New York, 47-49.

Erdèyi, A., Magnus, W., Oberhettinger, F. and Tricomi, F.G, (1954), *Tables of Integral Transforms,* **1,** Mcgraw-Hill, New York, 8, 14, 64 and 72.

Hsu, H.P. (1970), *Fourier Analysis,* Simon and Schuster, New York 107 and 119.

Karasudhi, P. (1991), *Foundations of Solid Mechanics,* Kluwer Academic Publishers, Dordrecht, The Netherlands, 197-203, 269-270 and 318-348.

Karasudhi, P. and Liu Y.C. (1992), "Far-field waves in elastic and viscoelastic spaces", *Recent Advances in Structural Mechanics-1992,* edited by Kwon, Y.W. and Chung, H.H., *ASME PVP*-Vol. 248/*NE***10.** 93-99.

Keer, L.M., Jabali, H.H. and Chantaramungkorn, K. (1974), "Torsional oscillation of a layer bonded to an elastic half-space". *Int. J. Solids Structures,* **10,** 1-13.

Koppe, H. (1948), "Über Rayleigh-Wellen and der Oberfläche zweier Medien", *Z. angew, Math. Mech.,* **28,** 355-360.

Liu, Y.C. (1992), "An infinite element algorithm for vibration of elastic and viscoelastic half spaces", *D. Eng. Dissertation,* Asian Institute of Technology, Bangkok, Thailand.

Luco, J.E. (1974), "Inpedance functions for a rigid foundation on a layered medium", *Nucl. Eng. Des.*, **31,** 204-207.

Luco, J.E. (1976a), "Torsional response of structures for SH Waves: The case of hemispherical foundations", *Bull, Seismological Soc. America,* **66** (1), 109-124.

Luco, J.E. (1976b), "Vibrations of a rigid disc on a layered viscoelastic medium", *Nucl. Eng. Des.*, **36,** 325-340.

Luco, J.E. and Westmann, R.A. (1971), "Dynamic response of circular footings," *J. Eng. Mech, ASCE,* **5,** 1381-1395

Luco, J.E. and Westmann, R.A. (1972), "Dynamic response of a rigid footing bonded to an elastic half-space", *J. Appl. Mech.*, **39,** 527-534.

Mita, A. and Luco, J.E. (1987), "Dynamic response of embedded foundations: A hybrid approach", *Comput. Meths. Appl. Mech. Engrg.*, **63,** 233-259.

Rajapakse, R.K.N.D. and Karasudhi, P. (1986), "An efficient elastodynamic infinite element", *Int. J. Solids Structures,* **22,** No. 6, 643-657.

Stoneley, R. (1924), "Elastic waves at the surface of separation of two solids", *Proc. Roy. Soc. (London), A,* **106,** 416-428.

Veletsos, A.S. and Nair, V.V.D (1974), "Torsional vibration of viscoelastic foundation", *J. Geotech. Eng., ASCE,* **100,** 225-246.

Veletsos, A.S. and Verbic, B. (1973), "Vibration of viscoelastic foundation", *Earthquake Eng. Struct. Dyn.*, **2,** 87-102.

Veletsos, A.S. and Wei, Y.T. (1971), "Lateral and rocking vibrations of footings", *J. Soil Mech. Foundations, ASCE,* **97** (SM9), 1227-1248.

Zhang, C.H. and Zhao, C.B. (1987), "Coupling method of finite and infinite elements for strip foundation wave problems", *Earthquake Eng. Struct. Dyn.* **15,** 839-851.